ELSEVIER

Physica A 249 (1998) 184–189

PHYSICA A

Stick–slip dynamics of interfacial friction

M.G. Rozman [a], M. Urbakh [b,*], J. Klafter [b]

[a] Institute of Physics, Riia 142, EE2400 Tartu, Estonia

[b] School of Chemistry, Tel Aviv University, 69978 Tel Aviv, Israel

Abstract

We investigate a model system which consists of a chain of particles that interact with two periodic potentials representing two confining plates, one of which is externally driven. The model leads to a spectrum of rich behaviors in the motion of the top driven plate: stick–slip, intermittent kinetic regime, characterized by force fluctuations, and two types of sliding above a critical driving velocity v_c. Similar behaviors are typical of a broad range of systems including thin sheared liquids. The relaxation of the "slip" part between two "stick" events in the stick–slip time series may display more than one characteristic time scale. The different relaxation times are shown to be related to a velocity-dependent effective frictional force felt by the driven plate.

1. Introduction

Sheared liquids confined between two atomically smooth solid surfaces display a spectrum of behaviors which include stick–slip motion followed, as the relative velocity of the plates increases, by intermittent and smooth motions [1–3]. Different models have been proposed to account for these types of motion including spring-block models [4], chains adsorbed on a substrate [5], models with melting–freezing transitions [6,7] and an embedded-particle model [8,9].

However, the origin of stick–slip motion and the related phenomena are still unclear and under some debate. Experimentally, it has been observed [10] that, under overdamped conditions, "slip" relaxation manifests more than one characteristic time scale. Typically, a sharp decrease at early times is followed by a tail of a slow decay. Phenomenological theoretical studies [6,7] have related the stick–slip behavior to a dynamical phase transition [6], or to a velocity-dependent frictional force [7].

In this paper we discuss a *microscopic model* which leads to the observed behavior [10] and to predictions that are amenable to experimental tests.

* Corresponding author.

PII S0378-4371(97)00462-7

2. The model

We extend the model [8,9] of a single particle that interacts with two periodic potentials that represent two confining plates, one of which is externally driven, to include an embedded chain of particles (Fig. 1). Consider a one-dimensional system of two rigid plates and a chain of particles embedded between them. The top plate of mass M is pulled by a linear spring with a spring constant K connected to a stage which moves with a velocity $\mathscr{V}$.

The equations of motion for the top plate and chain particles are

$$M\ddot{X} + \sum_{i=1}^{N} \eta(\dot{X} - \dot{x}_i) + K(X - \mathscr{V}t) + \sum_{i=1}^{N} \frac{\partial U(x_i - X)}{\partial X} = 0\,, \tag{1}$$

$$m\ddot{x}_i + \eta(2\dot{x}_i - \dot{X}) + \sum_{j \neq i} \frac{\partial V(x_i - x_j)}{\partial x_j} + \frac{\partial U(x_i)}{\partial x_i} + \frac{\partial U(x_i - X)}{\partial x_i} = 0\,, \tag{2}$$

where N is the number of particles in the chain, x_i ($i = 1,\ldots,N$) and X are the coordinates of chain particles and the top plate, respectively, and m is the mass of each particle. The second terms in Eqs. (1) and (2) describe the dissipative forces between the particle and the plates, which are proportional to their relative velocities. These terms account for dissipation which arises from interaction with phonons and/or other excitations. The third term in Eq. (1) is the driving force due to the stage motion. The remaining terms originate from the spatially periodic interaction between the particle and the plates, $U(x)$, and from the inter-particle interactions within the chain, $V(x_i - x_j)$. There is no direct interaction between the plates. In the present work we choose $U(x) = -U_0 \cos(2\pi x/b)$, where b is the spatial period of the particle–plate interaction potential; inter-particle potential is assumed to be harmonic with nearest-neighbor interactions only, $V(x_i - x_{i\pm1}) = k(x_i - x_{i\pm1} \mp a)^2/2$. Here k is the elastic chain constant, and a is the equilibrium spacing between particles in a free chain.

Let us introduce the following dimensionless variables and parameters: the coordinate $y = x/b$ and the time $\tau = \omega t$, where $\omega = (2\pi/b)(U_0/m)^{1/2}$ is the frequency of the small oscillations of the particle in the minima of the potential $U(x)$; $\gamma = \eta/(m\omega)$ which is a dimensionless friction constant, $\varepsilon = m/M$ the ratio of particle and plate masses, $\alpha = \Omega/\omega$ the ratio of frequencies of the free oscillations of the top plate $\Omega = (K/M)^{1/2}$ and the particle, $\delta = (b-a)/b$ the misfit of the substrate and chain periods and $v = (\omega_{ch}/\omega)^2$ the ratio of the frequencies related to interparticle and particle–plate interactions; here $\omega_{ch} = (k/m)^{1/2}$ is the characteristic frequency of the chain.

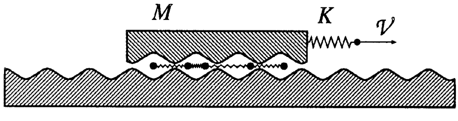

Fig. 1. Schematic sketch of the model geometry.

Generally, the stick–slip dynamics of the chain model is characterized by a chaotic behavior of the top plate and the embedded particles. In this article we focus only on the range of low stage velocities, where the motion is close to periodic.

3. Results

The chain model introduced above exhibits similar behavior previously observed in the single-particle model [8,9]. Again the motion of the top plate, which is the experimental observable, shows stick–slip, intermittent and sliding regimes. Here, however, we notice vibrational fluctuations typical of the chain which superimpose on the corresponding single particle behavior. Fig. 2 demonstrates the possibility that changes in the sliding phase can be accompanied by changes in the chain length. Shown are motion in a stretched state of the chain in one phase and in a free state in the other phase.

We concentrate below on the stick–slip regime typical to low driving stage velocities, and analyze a time window which corresponds to "slip" motion between two "stick" events. Namely, just as the top plate overcomes the static friction and starts moving, dissipation sets in and the plate relaxes toward another stick event. This slip relaxation pattern depends on the conditions under which the stick–slip motion is being studied. In the present work we consider the *overdamped* case, where the characteristic slip time is much longer than the response time of the mechanical system $\sim 2\pi\sqrt{M/K}$. The overdamped regime is realized experimentally if the spring constant K is sufficiently weak, and/or if the friction constant η is large. In numerical calculations we use the following values of parameters: $\varepsilon = 1/125$, $\gamma = 0.3$, $N = 15$, $\delta = 0.1$, $\rho = 1.0$.

Figs. 3a and 3b display the time evolution of the spring force and of the top-plate velocity during the slip motion. One clearly notices more than one time scale

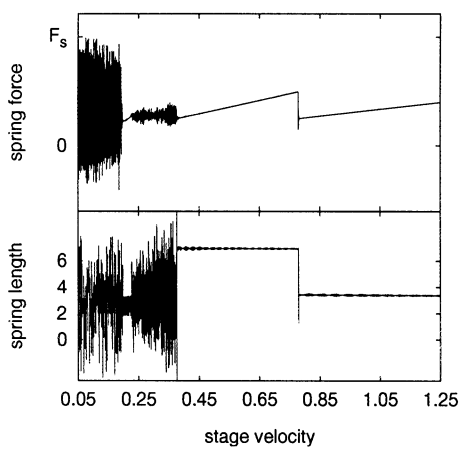

Fig. 2. Time variations of the spring force and the chain length for the case where the driving stage moves with a small constant acceleration. $\alpha = 0.02$, $\gamma = 0.1$, $\varepsilon = 0.125$, $N = 5$, $\delta = 0.2$, $v = 0.1$.

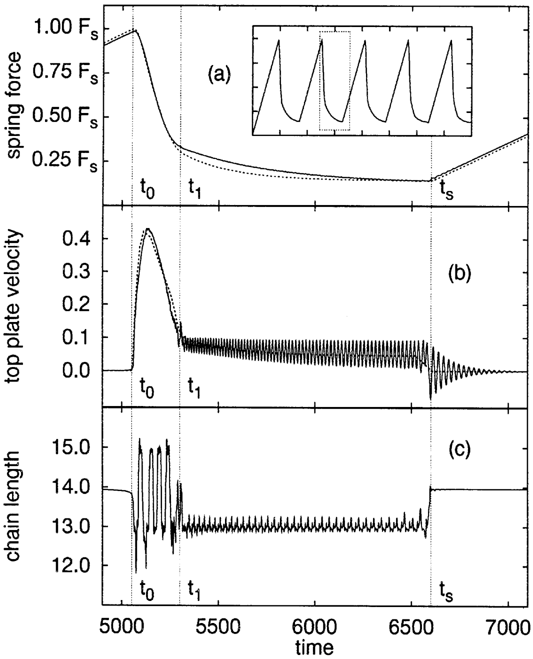

Fig. 3. Time evolution of the spring force (a), top plate velocity (b), and length of the embedded chain (c), during slip relaxation. Solid lines are the results of simulations, dashed lines in (a) and (b) correspond to the effective force approximation, Eq. (3). Inset shows a stick–slip time series with a window which indicates the time interval presented in (a)–(c). In dimensionless units stage velocity $\mathscr{V}/(\omega b) = 0.046$, and spring constant $\alpha = 0.015$.

in the relaxation process. The behaviors observed for the spring force and the top-plate velocity appear also in the properties of the chain. The chain length [Fig. 3(c)] shows two distinctive regimes: strong fluctuations for $t_0 < t < t_1$ and quasi-periodic oscillations around a stretched state for $t_1 < t < t_s$.

In order to provide a coarse-grained picture of the top-plate motion, which is the basic observable, we use an approximate description [9] based on a separation to "slow" and "fast" motions of the system. We describe the slow system motion in terms of an effective velocity-dependent force that acts on the top plate

$$M\ddot{X} + F(\dot{X}) + K(X - \mathscr{V}t) = 0 \,. \tag{3}$$

The effective force $F(v)$ is calculated by assuming that the top-plate moves with the constant velocity, and by averaging the potential and dissipative components of the friction over the fast fluctuations of the top-plate motion [8,9].

In Fig. 4 we present the effective force $F(v)$ which displays three different regimes: (1) At high plate velocity, $v > v_{\rm th}$, the chain decouples from the plates and moves with a velocity $v/2$. (2) At intermediate velocities, $v^* < v < v_{\rm th}$ the chain is trapped by one of the plates and each particle performs small oscillations around the corresponding

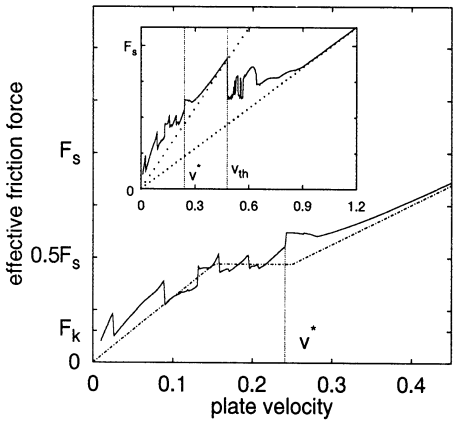

Fig. 4. Effective frictional force acting on the top plate as a function of plate velocity. Dashed-dotted line shows the smoothed force used for the approximate description according to Eq. (3). Dotted lines with slopes $N\gamma$ and $N\gamma/2$ are presented in the inset for reference.

minimum of the particle–plate interaction potential. (3) At low velocities, $v < v^*$, the center mass of the chain again moves with the velocity $v/2$, but its length strongly fluctuates.

In order to simulate the motion of the top plate, the effective force should be supplemented by the static friction F_s and kinetic friction F_k. The former is the largest depinning force [9] and the latter is the minimal force necessary to keep the plate sliding at low velocities. The static friction is determined by the potential interaction between the plates and the chain, and the kinetic friction has a dissipative nature. Neither F_s nor F_k are included in the effective force found by the time averaging.

Velocity-dependent forces with features similar to those found here have been postulated to mimic the motion of the top plate in stick–slip experiments [10,7]. Here we calculate $F(v)$ directly from the model. In Fig. 3 we fit the spring force and top plate velocity, obtained through the solution of Eq. (3), to the solution of the model (Eqs. (1) and (2)).

Introducing the effective force $F(v)$ makes it possible to relate the two time intervals in the slip relaxation (Fig. 3) to the nature of $F(v)$. Basically, the relaxation pattern should depend on the maximum value of the velocity reached by the top plate. For our choice of parameters the maximum of the plate velocity lies in the range $v^* < v_{\max} < v_{\mathrm{th}}$. The relaxation process probes therefore only those phases that correspond to $v < v_{\mathrm{th}}$. Namely, only two regimes are to be expected. Indeed the initial part of the slip relaxation (or top-plate velocity) results from the frictional force in the range $v^* < v < v_{\mathrm{th}}$, and the longer time relaxation results from $F(v)$ in the range $v < v^*$. Both the time dependence and the amplitude of the slip relaxation predicted here are consistent with the experimentally observed behavior [10].

For other choices of parameters, for which the maximum of the top-plate velocity lies in the range $v > v_{\mathrm{th}}$, the relaxation probes all three characteristic ranges of $F(v)$ leading to relaxation pattern with three distinct time scales.

The observed temporal behavior of the slip part depends on how broad is the probed range of the effective force $F(v)$. Namely, by changing the spring constant K one can control the experimentally observed relaxation pattern of the slip: one, two or three types of relaxation.

Acknowledgements

Financial support for this work by the Israel Science Foundation is gratefully acknowledged. M.R. acknowledges the support of the Alexander von Humboldt Stiftung and the Estonian Science Foundation under the grant No. 2689.

References

[1] H. Yoshizawa, P. McGuiggan, J. Israelachvili, Science 259 (1993) 1305.
[2] G. Reiter, L. Demirel, S. Granick, Science 263 (1994) 1741.
[3] P.A. Thompson, M.O. Robbins, G.S. Grest, Israel J. Chem. 35 (1995) 93.
[4] J.M. Carlson, J.S. Langer, B.E. Shaw, Rev. Mod. Phys. 66 (1994) 657.
[5] Y. Braiman, F. Family, G. Hentschel, Phys. Rev. E 53 (1996) R3005.
[6] J.M. Carlson, A.A. Batista, Phys. Rev. E 53 (1996) 4153.
[7] B.N.J. Persson, Phys. Rev. B 50 (1994) 4771.
[8] M.G. Rozman, M. Urbakh, J. Klafter, Phys. Rev. Lett. 77 (1996) 683.
[9] M.G. Rozman, M. Urbakh, J. Klafter, Phys. Rev. E 54 (1996) 6485.
[10] A.D. Berman, W.A. Ducker, J.N. Israelachvili, Langmuir 12 (1996) 4559.